ADVANCED MATERIALS
www.advmat.de

Conductive Ink with Circular Life Cycle for Printed Electronics

*Junpyo Kwon, Christopher DelRe, Philjun Kang, Aaron Hall, Daniel Arnold, Ivan Jayapurna, Le Ma, Matthew Michalek, Robert O. Ritchie, and Ting Xu**

Electronic waste carries energetic costs and an environmental burden rivaling that of plastic waste due to the rarity and toxicity of the heavy-metal components. Recyclable conductive composites are introduced for printed circuits formulated with polycaprolactone (PCL), conductive fillers, and enzyme/protectant nanoclusters. Circuits can be printed with flexibility (breaking strain ≈80%) and conductivity (≈2.1×10^4 S m^{-1}). These composites are degraded at the end of life by immersion in warm water with programmable latency. Approximately 94% of the functional fillers can be recycled and reused with similar device performance. The printed circuits remain functional and degradable after shelf storage for at least 7 months at room temperature and one month of continuous operation under electrical voltage. The present studies provide composite design toward recyclable and easily disposable printed electronics for applications such as wearable electronics, biosensors, and soft robotics.

1. Introduction

Unrecycled materials at the end of life impose a significant environmental and economic burden due to pollution buildup and loss of valuable resources.[1] Given the rapid and increasing turnover rate of electronic products, electronic waste (e-waste) containing toxic substances[2] and precious metals[3] is a pressing environmental, safety, and economic concern.[4] Yet, the recyclability of electronics is rarely a design criterion, and existing recycling procedures lead to secondary pollution and insufficient recovery of precious components.[5]

Transient electronics[6] are programmed with operational lifetimes and on-demand transformation.[7] Stimuli-responsiveness can be engineered in the protection layers to control the device's lifetime. Several layers need to be degraded using combined stimili including heat, ionic species, and UV light.[8] While these multilayer materials are successful for electronics, their complexity may increase processing costs and present barriers to e-waste recycling using existing infrastructure. Embedding enzyme nanoclusters into plastics[9] can program the degradations of polyesters under industrial composting conditions. Integrating these new developments in composite materials may serve as the ideal entry point toward sustainable printed electronics and e-waste reduction.

Degradable composites can provide opportunities to engineer conductive inks to fabricate flexible electronic circuits (**Scheme 1**). When formulated using conductive filler, biodegradable polymer binder, and enzymes,the composite ink is mechanically robust with a tensile strength of ≈6.3 MPa and exhibits mechanical flexibility with ≈80% strain at break and electrical conductivity of ≈2.1×10^4 S m^{-1}. The printed circuits at the end of life are degraded by submerging in warm water, and the degradation rate and latency can be programed by thermal treatments. The metal fillers were collected and reused with no observable loss in function. The circuits remain fully functional and degradable after 7 months of storage and 1 month of continuous operation under 3 V electrical voltage at room temperature without humidity control. Furthermore, the process is optimized to be compatible with commercially sourced enzymes without purification, a significant step forward toward scalable device fabrication.

2. Results and Discussion

Commercially available enzymes are more cost-effective but contain undefined stabilizers. Previous studies in enzyme-containing plastics focused on degradation mechanisms and used purified enzymes.[9a,c] This significantly limits the scalability

J. Kwon, R. O. Ritchie
Department of Mechanical Engineering
University of California, Berkeley
Berkeley, CA 94720, USA

J. Kwon, C. DelRe, L. Ma, R. O. Ritchie, T. Xu
Materials Sciences Division
Lawrence Berkeley National Laboratory
Berkeley, CA 94720, USA
E-mail: tingxu@berkeley.edu

C. DelRe, A. Hall, I. Jayapurna, L. Ma, M. Michalek, R. O. Ritchie, T. Xu
Department of Materials Science and Engineering
University of California, Berkeley
Berkeley, CA 94720, USA

P. Kang, T. Xu
Department of Chemistry
University of California, Berkeley
Berkeley, CA 94720, USA

D. Arnold
Department of Chemical Engineering
University of California, Berkeley
Berkeley, CA 94720, USA

The ORCID identification number(s) for the author(s) of this article can be found under https://doi.org/10.1002/adma.202202177.

DOI: 10.1002/adma.202202177

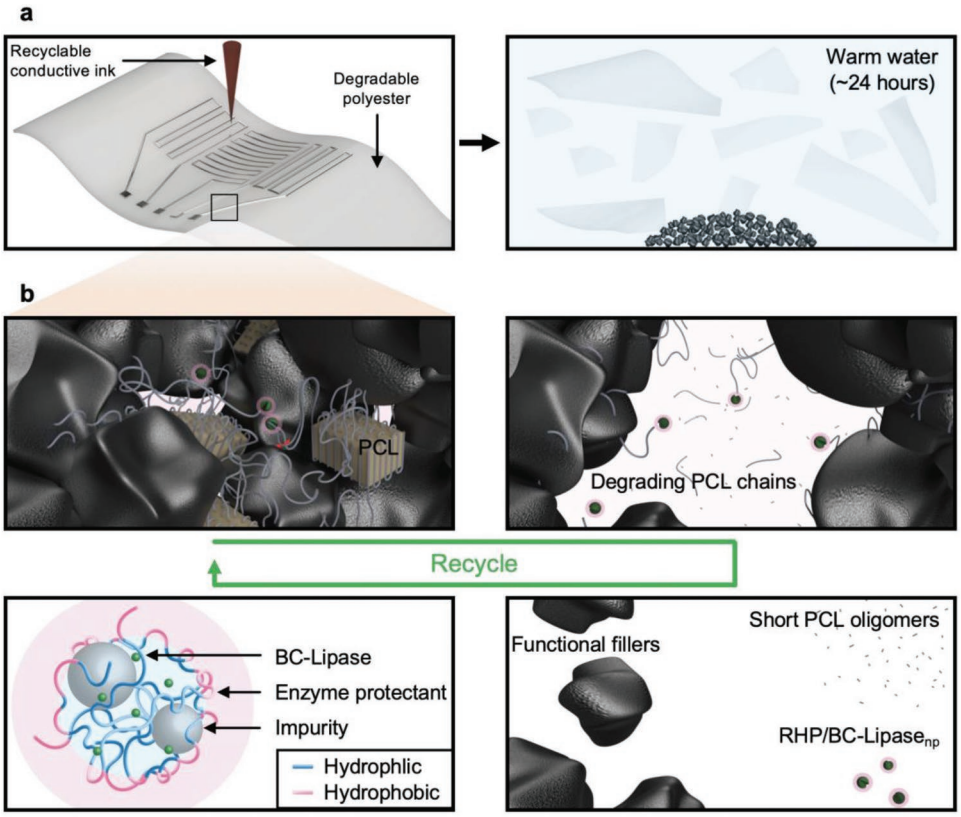

Scheme 1. The recycling mechanism of the printed circuits using RHP/BC-Lipase$_{np}$ nanoclusters. a) Flexible electronic circuits fabricated by 3D printing or direct ink writing. The circuits can be disintegrated in warm water, and the separated fillers can be recollected. b) The conductive ink including functional fillers, PCL, and RHP/BC-Lipase$_{np}$. The PCL binder (represented by gray chains) degrades through enzyme-induced chain scission in warm water. RHP/BC-Lipase$_{np}$ includes BC-Lipase (green), enzyme protectant (RHPs) highlighting the hydrophilic (blue) and the hydrophobic (pink) segments, and impurities (gray spheres).

and increases cost. The enzyme cocktail (BC-Lipase$_{np}$) purchased directly from Sigma-Aldrich contains both enzymes and stabilizers, as shown in **Figure 1**a and Figure S1 in the Supporting Information. Random heteropolymers (RHPs) are used to stabilize and disperse enzymes within polymeric matrices. This process relies on the enzyme/RHP complexation. We hypothesized that RHPs that have more pairs of favorable interactions with enzymes can compete with the interactions between the enzymes and commercial stabilizers. Thus, we first screened RHPs as a function of molecular weights.

The molecular weight (MW) of RHPs affects the apparent catalytic performance of embedded BC-Lipase$_{np}$. Low MW RHPs act as additives and influence the morphology of the polymer matrix, limiting chain-end accessibility of the embedded enzymes which reduces the polymer-to-monomer conversion.[9a] High MW RHPs may better complex with proteins via multivalent interactions to enhance activity retention and dispersion. Thus, RHPs with the same monomer composition but different MWs (69, 81, and 127 kDa) were tested. The composite films composed of polycaprolactone (PCL) and RHP-enzyme complexes (PCL/RHP/BC-Lipase$_{np}$) were prepared under the same conditions and immersed in warm water (37 °C) for 24 h (Figure 1b). The films with 69 kDa RHP exhibited 65.9% (±8.4%) weight loss. The films with 127 kDa RHP showed 80.0% (±16.7%) weight loss under the same experimental conditions. Although the films prepared with purified BC-Lipase showed the highest degradation rates displaying 91.5% (±1.6%) weight loss over 24 h, the 127 kDa RHP with the unpurified enzyme blend was chosen for subsequent studies to ensure scalability (Figure 1c).

Silver (Ag) flakes were blended as a conductive filler to impart electrical conductivity. When Ag/PCL (filler load ≈80 wt%) was mixed with fluorescently labeled RHP/BC-Lipase$_{np}$, fluorescence microscopy confirmed that the enzymes were homogeneously dispersed in the PCL matrix (**Figure 2**a). After ≈80 h of immersion in warm water (37 °C), the Ag flakes precipitated at the bottom of the container. The reclaimed Ag flakes showed a morphology similar to the virgin material under optical microscopy (Figure S5, Supporting Information). Thermogravimetric analysis (TGA) (Figure 2b) confirmed that the recovered Ag flakes had a purity greater than 94% with less than 6% of organic material absorbed. The process can be repeated multiple times and the conductivity of the ink based on the recycled Ag flakes remains similar to that of the as-purchased material (Figure 2c).

The electrical conductivity of the ink (PCL/Ag/RHP/BC-Lipase$_{np}$) increased logarithmically as the volume fraction of Ag flakes was increased from 10 to 30 vol% (Figure S6, Supporting Information), which is consistent with the percolation theory[10] and previous composite studies.[11] Upon further increasing the volume fraction of Ag flakes, the conductivity

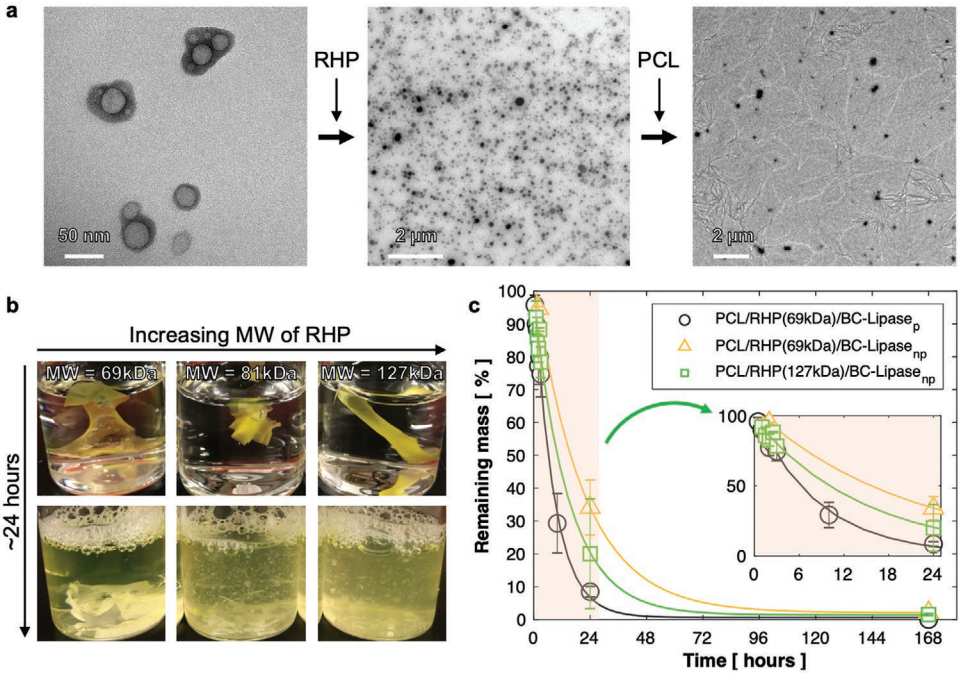

Figure 1. The PCL binder with nanoscopically dispersed RHP/BC-Lipase$_{np}$ with the degradation performance affected by the molecular weight of the RHPs. a) TEM images of the nonpurified enzyme complex in water, RHP/BC-Lipase$_{np}$, and PCL/RHP/BC-Lipase$_{np}$. b) The degradation results for PCL/RHP/BC-Lipase$_{np}$ with the different molecular weights of RHPs (69, 81, and 127 kDa). The fluorescently labeled BC-Lipase$_{np}$ was used for color contrast. c) Degradation profiles of PCL with purified BC-Lipase (PCL/RHP(69 kDa)/BC-Lipase$_p$) and with nonpurified BC-Lipase (BC-Lipase$_{np}$) that was embedded with either 69 or 127 kDa RHP (sample size, $n = 3$).

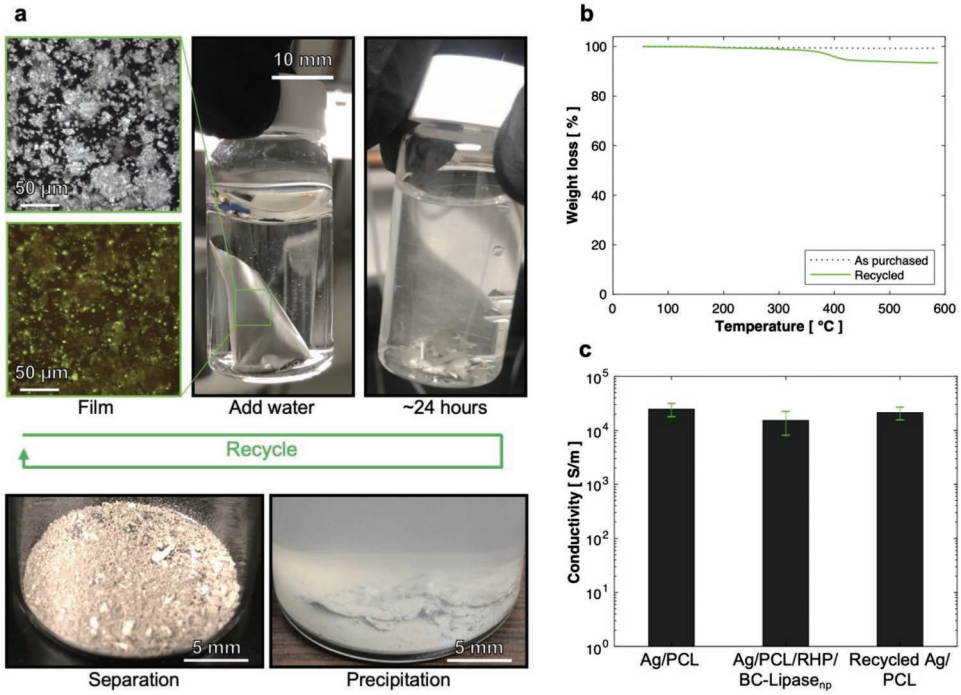

Figure 2. E-waste recycling. a) Recycling process of metal fillers by enzyme-catalyzed degradation. A dry-cast Ag/PCL/RHP/BC-Lipase$_{np}$ film was placed in a warm buffer (37 °C). Optical microscopy image of the ink (≈80 wt% of Ag flakes) and fluorescence microscopy image of the ink with fluorescently labeled BC-Lipase$_{np}$. After the degradation (≈24 h), Ag flakes were precipitated and recollected for recycling. b) TGA of the recycled and as purchased Ag flakes. c) Comparison of the electrical conductivity of composites with and without enzyme clusters and with recycled Ag flakes (78.9 wt%).

slightly improved until a plateau was observed between 30 and 35 vol%. Cross-sectional scanning electron microscopy (SEM) analysis validated the formation of a continuous conducting network of Ag flakes. Thus, the optimized ink was formulated with 30 vol% (78.9 wt%) Ag flakes for subsequent studies. The composite's conductivity is 2.1×10^4 S m^{-1} and meets the requirements for electronics.[8] The results of uniaxial tensile tests, given in Figure S7 (Supporting Information), show the engineering stress–strain curve of a tensile dog-bone composite specimen composite following ASTM Standard D1708. The composite displayed a maximum tensile strength of 6.3 MPa with a tensile ductility, i.e., the strain at break, of ≈80%. Hence, the composite composed of 78.9 wt% Ag flakes showed both adequate electrical conductivity and mechanical robustness.

Chemical and thermal stabilities are required to ensure stable operation during material usage.[12] The stabilities of the PCL matrix and the composite ink with high concentrations of Ag flakes (78.9 wt%) were tested. Fourier transform infrared spectroscopy (FT-IR) was used to confirm the chemical integrity of the PCL binders before and after adding Ag/RHP/BC-Lipase$_{np}$. As shown in Figure S8 (Supporting Information), PCL shows the main characteristic peaks of ester group that appear at 1720 cm^{-1} corresponding to the stretching of C=O and 1294, 1240, and 1184 cm^{-1} corresponding to the stretching of C–O–C.[13] These characteristic peaks were observed in the spectra of PCL/Ag/RHP/BC-Lipase$_{np}$ and no additional peaks or broadening bands were seen.

TGA was carried out at 25 to 600 °C to evaluate the composite's thermal stability and to confirm the filler ratios. Figure S9 (Supporting Information) shows the weight loss curves of the PCL and PCL/Ag/RHP/BC-Lipase$_{np}$. Pure PCL starts to thermally decompose around 370 °C and is completely decomposed around 400 °C. The composite began to decompose near 390 °C with a weight loss of ≈80% up to 400 °C. The increased polymer/filler interaction may enhance the onset decomposition temperature of PCL/Ag/RHP/BC-Lipase$_{np}$.[14] This also might affect the enzymatic degradability.[9c] To further investigate, differential scanning calorimetry (DSC) was performed to study how the added Ag fillers could affect the PCL crystallization. There was an increase in melting temperature from 58 °C ± 1.2 °C to 59 °C ± 0.7 °C. The lamellae thickness of the PCL only increases slightly with the presence of the Ag flakes (Figure S10, Supporting Information).

We tested the degradability of the composites after exposure to electric fields to evaluate possible charge-induced denaturation of the embedded enzymes. The enzyme's activity was monitored by the collapse of the percolated metallic filler networks, leading to electrical conductivity loss (Figure S11, Supporting Information). **Figure 3**a and Video S2 (Supporting Information) show that Ag/PCL does not show any current change when submerged in warm water (37 °C), whereas the conductivity of Ag/PCL/RHP/BC-Lipase$_{np}$ decreases with time. The surfaces of both tested circuits were characterized using SEM (Figure 3b). The circuit without RHP/BC-Lipase$_{np}$ did not show significant morphological change. However, the circuits based on the PCL/Ag/RHP/BC-Lipase$_{np}$ composite were disintegrated due to the enzymatic depolymerization of the PCL chains in percolating networks of Ag flakes. The selective biodegradation of PCL chains can be fully employed to recycle different types of fillers. Figure S12 (Supporting Information) shows that the degradable composite design is still valid under 50 V with carbon black as the conductive filler, which offers diverse filler selections based on user preferences.

The circuits remained degradable after storage in ambient conditions for seven months, followed by up to 31 d of continuous operation under a load of 3 V (Figure S13, Supporting Information). The RHPs modulate the local microenvironment for the enzymes and are one key factor in retaining degradability over a long storage period and under electrical voltage. Confining RHP/BC-Lipase$_{np}$ in a polymer matrix also increases its stability by restricting the enzyme's translational and conformational mobility. Furthermore, the operating voltage (3–50 V) is much lower than the voltage that affects the forces involved in the 3D structure and conformation of lipase (>5 kV).[15] The size of the enzyme-RHP clusters (hydrodynamic diameter $d_h > 300$ nm) (Figure S2, Supporting Information) is larger than the typical electron tunneling distance (a few nanometers),[16] which likely prevents voltage-induced denaturation while the material is in operation.

Stable operation is crucial for electronics with a programmable lifecycle. By relying on enzyme-catalyzed depolymerization to breakdown the circuits, the hydrolysis rate can be controlled by degrading temperature. At temperatures below ≈30 °C, no degradation occurs because the hindered enzyme and polymer mobility prevent substrate binding and subsequent depolymerization. However, upon increasing the temperature to 41 °C, degradation significantly accelerates as observed from the analysis of gel permeation chromatography (GPC) measurements (Figure 3c). This is due to the enhanced chain mobility and thermodynamic driving force for crystalline segments to be "pulled" from their lamellae.[9c]

In addition, the chain-end mediated degradation of PCL chains can be controlled by increasing the lamellae thickness of the PCL matrix through thermal annealing. Accordingly, the printed circuit was thermally annealed and crystallized at 49 °C.[9c] As shown in Figure 3d, DSC confirms a respective ≈10% and ≈6 °C increase in crystallinity and melting temperature of the thermally annealed circuits. The increased melting temperature corresponded to a thicker crystalline lamellae and reduced PCL's degradation rate (Figure 3e). It also required a higher onset temperature (≈49 °C) to trigger the degradation. Thus, controlling the binder's crystalline properties can be exploited to tune degradation rates to ensure degradation latency in different user environments.

The ink can be printed on various substrates, such as glasses, rubbers, living plants, and degradable polyesters (**Figure 4**). As the printed materials are designed to have mechanical flexibility and electrical conductivity, their mechanical deformation can be detected from monotonic conductivity changes in cyclic stretching tests (1000 times and 1 cycle s^{-1}) (Figure S14, Supporting Information). The composite can also be fabricated using hot-melt extrusion. In this work, the ink was prepared by melt blending of PCL/RHP/BC-Lipase$_{np}$ and 79.8 wt% Ag flakes at under 60 °C for less than 5 min and subsequently extruded using a syringe without using any organic solvents. The melt-extruded filament also exhibited good electrical conductivity and degraded when immersed in warm water (Figure S15, Supporting Information).

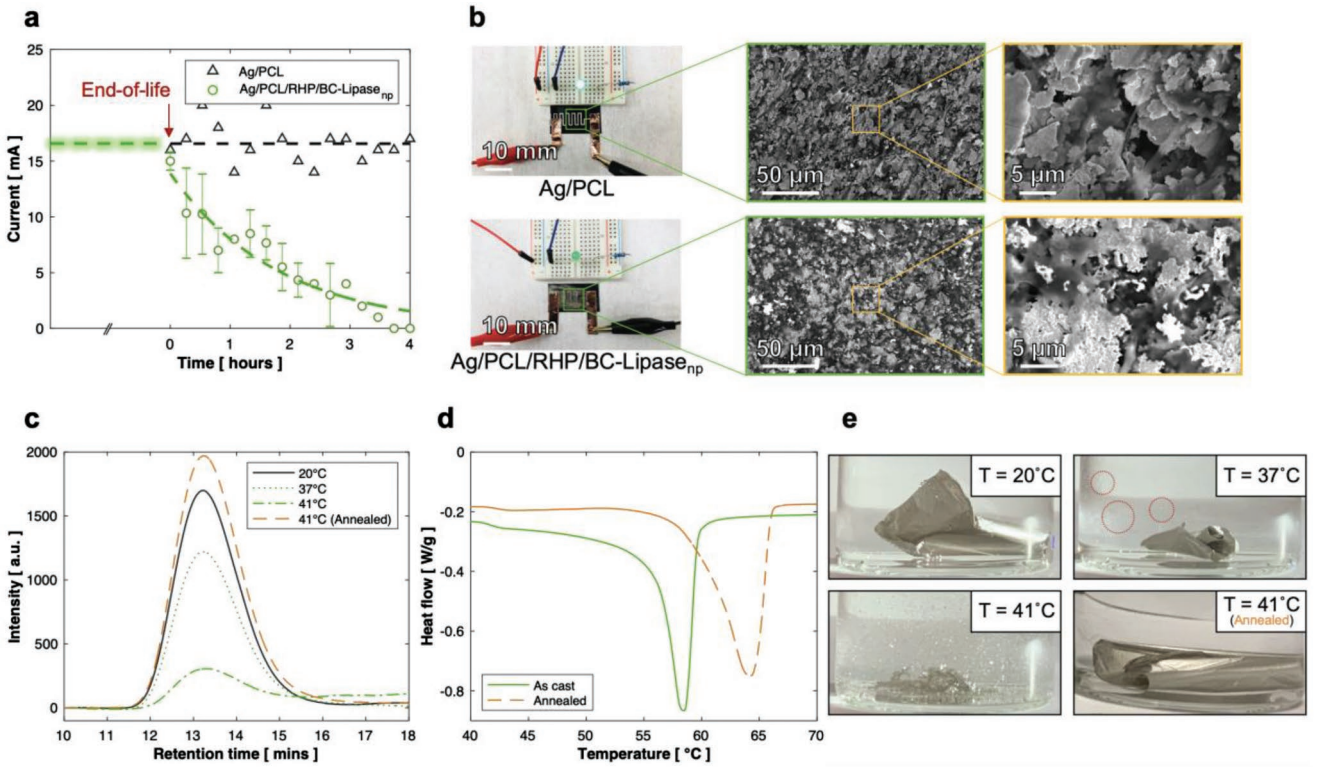

Figure 3. Degradation tests under electrical voltage. a) The enzymatic degradation under a 5 V potential of Ag/PCL/RHP/BC-Lipase$_{np}$ over time, triggered by warm water. The circuits are conductive under ambient conditions at room temperature for 1 month or underwater (20 °C). When the degradation begins by increasing the water temperature to 37 °C, the measured electrical currents decrease as the PCL degrades, showing that the activity of BC-Lipase is not compromised under an electrical potential. Statistical values were measured from four independent measurements. b) SEM images of the printed circuits with and without RHP/BC-Lipase$_{np}$ after the degradation test. c) GPC results of Ag/PCL/RHP/BC-Lipase$_{np}$ and the thermally annealed film after degradation (≈24 h). The films were degraded as a function of water temperature (20, 37, and 41 °C). Mass loss results, estimated by integrating GPC peaks, show that the degradation rate is proportional to degradation temperature. d) DSC results of the as cast and annealed films. The thermal annealing process increased the crystallinity from 49.8% to 55.1%, as the melting enthalpy of 100% crystalline PCL was taken as 151.7 J g^{-1}.[18] e) The films in water after the degradations at various temperatures (≈24 h). Increased mass loss was observed with increasing temperature in as cast films, whereas annealed films remained intact even at 41 °C. The red circles indicate the silver particles dispersed in water.

We observed the significant reductions in adhesion strengths of the printed circuits after degradation (Figure S16 and Video S3, Supporting Information). This can be advantageous to disassemble and sort different components in e-wastes,[4a] such as circuits, resistors, capacitors, and batteries.[17] We performed lap-shear adhesion tests using flexible and stretchable substrates (Figure S17a, Supporting Information). The composite ink was evenly spread (5 × 5 mm) on one elastomer substrate, and another elastomer was pressed to form a lap junction. The as-cast ink has a failure force and displacement estimated to be 9.4 N (±1.0 N) and 18.2 mm (±5.0 mm), respectively. The set of the joints was immersed in warm water for 12 h and then dried overnight under ambient conditions. Post degradation treatment, the adhesion strength and displacement at failure decreased to 6.5 N (± 0.8 N) and 5.7 mm (±2.6 mm), respectively. All of the failures were characterized as cohesive failures, and a few defects could be identified from the fracture surfaces (Figure S17b, Supporting Information), indicating that the reduction in adhesion force was due to the degradation of the PCL matrix.

3. Conclusion

Non-purified BC-Lipase/RHP complexes were incorporated into Ag/PCL composites to create degradable electronic inks. The embedded enzymes catalyze the hydrolytic degradation of PCL chains in both films and printed states upon immersion in warm water. This RHP-assisted enzymatic depolymerization enables easy separation of electronic components and recycling of functional particles even after months of storage and use under ambient conditions. Furthermore, temperature and post-heat treatment can be used to modulate the polymer degradation rates after direct ink writing. As warm water is a main source to trigger the degradation and recycling, the proposed approach is more sustainable and potentially more cost-effective than the use of toxic and expensive organic solvents in recycling of e-waste made of multicomponents. These new biodegradable, recyclable, conductive, flexible, and printable materials can be applied across many electronic devices to serve as a cornerstone for the development of eco-friendly, recyclable electronics.

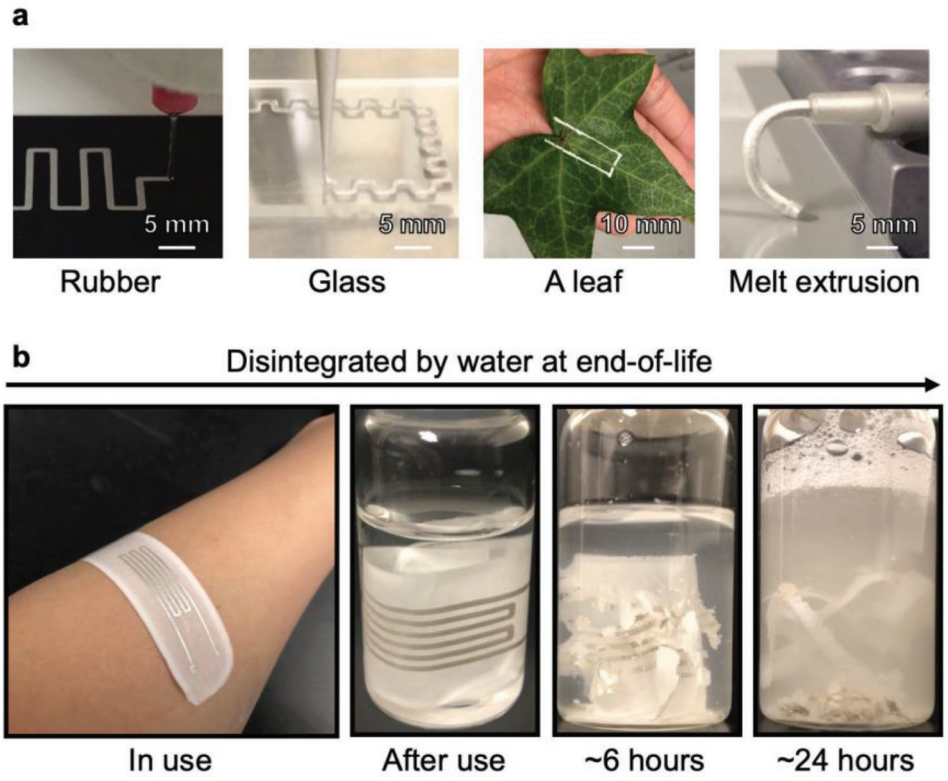

Figure 4. 3D printing applications. a) The ink printed on rubber, glass, and a leaf by direct ink writing. Ag flakes and RHP/BC-Lipase$_{np}$ were mixed in the PCL melt (≈60 °C), and then the mixture was extruded from a heated nozzle. b) The ink was printed on a PCL/RHP/BC-Lipase$_{np}$ substrate. The printed circuit disintegrates in warm water at the end of life.

4. Experimental Section

Materials: PCL (80 000 g mol^{-1}, PDI < 2) and Amano PS Lipase from *Burkholderia cepacia* were purchased from Sigma-Aldrich and Ag flakes from Inframat. The enzyme was dissolved in water and stored at −20 °C until use. Toluene (HPLC grade, >99.8% purity) and the salts to make the phosphate buffer (pH = 7.4) were purchased from Fisher Chemical. PCL (20 000 g mol^{-1}, PDI < 2) was used for the melt extrusion demonstration. The buffer was prepared with Milli-Q water, potassium chloride, and sodium chloride.

Ink Preparation: The random heteropolymer (RHP) was designed with four different monomers matching the chemically heterogeneous enzyme surfaces and synthesized as previously reported.[9b] The synthesized RHP was dissolved in water. Both BC-Lipase$_{np}$ and RHP water solutions were mixed together at room temperature for 5 min. The ratio RHP/BC-Lipase$_{np}$ was 2:1 by mass. The RHP/BC-Lipase$_{np}$ solution was dried in vacuo overnight. The dried RHP/BC-Lipase$_{np}$ was mixed with PCL-Toluene solution (100 mg mL^{-1}) and silver flakes for 5 min to produce the proper viscosity of the solution to be printed, and to allow for quick solvent evaporation. The mass ratio of RHP/BC-Lipase$_{np}$ and Ag/PCL ink was 98:2.

Direct Ink Writing (3D Printing): The Ag/PCL/RHP/BC-Lipase$_{np}$ ink was printed at room temperature with a three-axis motion-controlled stage (Aerotech) with the print paths generated with 3D robotic deposition software (Robocad 3.0). The diameter of the paths was set to 150–600 µm controlled by the size of the printing tips (EFD precision tips, EFD, East Providence, RI, USA); the extrusion of inks was controlled with an additional motor attached to the syringe. Toluene was selected as the printing solvent for its boiling point (110.6 °C) to prevent clogging of the nozzle, which can introduce defects or particle aggregations during the printing process.

Structural Characterization: Transmission electron microscopy (TEM) imaging was performed on a FEI Tecnai 12 microscope operating at a 120 kV accelerating voltage. Scanning electron microscopy (SEM) imaging was performed on a Hitachi S-5000 microscope. Scanning transmission electron microscopy energy-dispersive X-ray spectroscopy (STEM-EDS) was performed at the National Center for Electron Microscopy (NCEM) of the Molecular Foundry by using a FEI TitanX 60-300 microscope operated at 200 kV. The Bruker windowless EDS detector with a solid angle of 0.7 steradians enables high count rates with minimal dead time. The data were visualized with Esprit 1.9. Gel permeation chromatography (GPC) measurements were run using a total concentration of 2 mg mL^{-1} of the remaining Ag/PCL/RHP/BC-Lipase$_{np}$ film after the degradation (24 h) and a by-product in THF. 20 µL of the solution was injected into an Agilent PolyPore 7.5 × 300 mm column.

Mechanical Testing Characterization: Uniaxial tensile tests were performed on a screw-driven mechanical testing machine (Instron-5933, Norwood, MA, USA) with a 2 kN load cell. 300 µm films were cut into dog-bone samples with an ASTM D1708 cutting die; the specimen gauge lengths were set at 22 mm with the longitudinal strain calculated from the crosshead displacement. Testing was carried out at room temperature at a displacement rate of 10 mm min^{-1}. At least five samples of each condition were tested. Lap-shear tests were performed at a rate of 1 mm min^{-1} with two styrene–ethylene–butylene–styrene elastomer substrates (5 × 10 × 0.1 mm) and the ink (5 × 5 mm) between them after ≈12 h of degradation.

Thermal Characterization: Differential scanning calorimetry (DSC) (TA Instruments) measurements were performed at temperatures of 20–70 °C under nitrogen gas with a rate of 2 °C min^{-1}. Thermogravimetric analysis (TGA) (TA Instruments) measurements were performed at 25–600 °C with a rate of 20 °C min^{-1} in a nitrogen atmosphere.

Conductivity Measurement: A constant electrical potential of 5 V was applied using a DC power supply (E3612A, Agilent) and the buffer was heated to 37 °C using a silicon oil bath. The buffer level was kept constant with condensation controlled using a long tube glass. The

recycled silver flakes were washed once with toluene and dried at room temperature before measurements.

Statistical Analysis: The presented data were not preprocessed for statistical analysis. Statistical values, such as mean and standard deviations, were calculated from more than three independent experiments. MATLAB and ImageJ were used for the analysis.

Testing the Device on a Human Arm: The tests of the device on a human arm described in Figure 4b do not require Institutional Review Board (IRB) approval and has received the volunteer's consent. No identifiable private information or biospecimens of living individuals have been collected.

Supporting Information

Supporting Information is available from the Wiley Online Library or from the author.

Acknowledgements

This work was supported by the U.S. Department of Energy, Office of Science, Office of Basic Energy Sciences, Materials Sciences and Engineering Division (DOE-BES-MSE) under Contract DE-AC02-05-CH11231, through the Organic–Inorganic Nanocomposites KC3104 program. The US Department of Defense, Army Research Office support is under contract W911NF2110128 (Enzyme stabilization). T.X. conceived the idea and guided the project. J.K., C.D., and T.X. performed material characterization experiments, scalability studies, and analyzed degradation rates. J.K., A.D., and M.M. 3D printed the electronic circuits. J.K. and C.D. performed electron microscopy experiments and gel permeation chromatography characterizations. C.D. and L.M. performed transmission electron microscopy and energy-dispersive X-ray spectroscopy. J.K. and R.O.R. analyzed mechanical properties. P.K., A.H., and I.J. synthesized and characterized the RHPs.

Conflict of Interest

T.X., C.D., and J.K. filed a patent disclosure. A.H. is the founder and CEO of Intropic Materials.

Data Availability Statement

The data that support the findings of this study are available from the corresponding author upon reasonable request.

Keywords

3D printing, conductive ink, electronic waste, enzyme-containing composites, recycling

Received: March 8, 2022
Revised: May 11, 2022
Published online: June 11, 2022

[1] J. R. Jambeck, R. Geyer, C. Wilcox, T. R. Siegler, M. Perryman, A. Andrady, R. Narayan, K. L. Law, *Science* **2015**, *347*, 768.
[2] A. Islam, T. Ahmed, M. R. Awual, A. Rahman, M. Sultana, A. A. Aziz, M. U. Monir, S. H. Teo, M. Hasan, *J. Cleaner Prod.* **2020**, *244*, 118815.
[3] P. Kiddee, R. Naidu, M. H. Wong, *Waste Manage.* **2013**, *33*, 1237.
[4] a) A. Kumar, M. Holuszko, D. C. R. Espinosa, *Conserv. Recycl.* **2017**, *122*, 32; b) J. Cui, L. Zhang, *J. Hazard. Mater.* **2008**, *158*, 228.
[5] a) N. X. Williams, G. Bullard, N. Brooke, M. J. Therien, A. D. Franklin, *Nat. Electron.* **2021**, *4*, 261; b) W. B. Han, J. H. Lee, J.-W. Shin, S.-W. Hwang, *Adv. Mater.* **2020**, *32*, 2002211.
[6] S.-W. Hwang, H. Tao, D.-H. Kim, H. Cheng, J.-K. Song, E. Rill, M. A. Brenckle, B. Panilaitis, S. M. Won, Y.-S. Kim, Y. M. Song, K. J. Yu, A. Ameen, R. Li, Y. Su, M. Yang, D. L. Kaplan, M. R. Zakin, M. J. Slepian, Y. Huang, F. G. Omenetto, J. A. Rogers, *Science* **2012**, *337*, 1640.
[7] a) S. W. Hwang, S. K. Kang, X. Huang, M. A. Brenckle, F. G. Omenetto, J. A. Rogers, *Adv. Mater.* **2015**, *27*, 47; b) C. W. Park, S. K. Kang, H. L. Hernandez, J. A. Kaitz, D. S. Wie, J. Shin, O. P. Lee, N. R. Sottos, J. S. Moore, J. A. Rogers, *Adv. Mater.* **2015**, *27*, 3783; c) H. L. Hernandez, S. K. Kang, O. P. Lee, S. W. Hwang, J. A. Kaitz, B. Inci, C. W. Park, S. Chung, N. R. Sottos, J. S. Moore, *Adv. Mater.* **2014**, *26*, 7637.
[8] J. Shim, J. A. Rogers, S. Kang, *Mater. Sci. Eng., R* **2021**, *145*, 100624.
[9] a) C. DelRe, B. Chang, I. Jayapurna, A. Hall, A. Wang, K. Zolkin, T. Xu, *Adv. Mater.* **2021**, *33*, 2105707; b) B. Panganiban, B. Qiao, T. Jiang, C. DelRe, M. M. Obadia, T. D. Nguyen, A. A. Smith, A. Hall, I. Sit, M. G. Crosby, *Science* **2018**, *359*, 1239; c) C. DelRe, Y. Jiang, P. Kang, J. Kwon, A. Hall, I. Jayapurna, Z. Ruan, L. Ma, K. Zolkin, T. Li, C. D. Scown, R. O. Ritchie, T. P. Russell, T. Xu, *Nature* **2021**, *592*, 558.
[10] D. Stauffer, A. Aharony, *Introduction to Percolation Theory*, Taylor & Francis, London, UK **1994**.
[11] a) J. Kwon, K. Evans, M. Le, D. Arnold, M. E. Yildizdag, T. Zohdi, R. O. Ritchie, T. Xu, *ACS Appl. Mater. Interfaces* **2020**, *12*, 8687; b) A. D. Valentine, T. A. Busbee, J. W. Boley, J. R. Raney, A. Chortos, A. Kotikian, J. D. Berrigan, M. F. Durstock, J. A. Lewis, *Adv. Mater.* **2017**, *29*, 1703817.
[12] A. Cholewinski, P. Si, M. Uceda, M. Pope, B. Zhao, *Polymers* **2021**, *13*, 631.
[13] J. Si, Z. Cui, Q. Wang, Q. Liu, C. Liu, *Carbohydr. Polym.* **2016**, *143*, 270.
[14] D. Liu, G. Sui, Y. Dong, *Electrospun Polymers and Composites*, Woodhead Publishing, Sawston, UK **2021**, pp. 147–178.
[15] S. Y. Ho, G. S. Mittal, J. D. Cross, *J. Food Eng.* **1997**, *31*, 69.
[16] D. Toker, D. Azulay, N. Shimoni, I. Balberg, O. Millo, *Phys. Rev. B* **2003**, *68*, 041403.
[17] S. Zhang, E. Forssberg, *Conserv. Recycl.* **1997**, *21*, 247.
[18] A. Wurm, E. Zhuravlev, K. Eckstein, D. Jehnichen, D. Pospiech, R. Androsch, B. Wunderlich, C. Schick, *Macromolecules* **2012**, *45*, 3816.